DIFFRACTIVE DI-JET PRODUCTION AT HERA

Janos Zsembery
DAPNIA/SPP, CEA/Saclay
91191 Gif sur Yvette, France
Tel 33 1 69084555
FAX 33 1 69086428
E-mail: zsembery@hep.saclay.cea.fr

On behalf of the H1 and ZEUS collaborations

Differential dijet rates have been measured in interactions of the type ep→eXY at HERA by the H1 and ZEUS detectors. The component X of the hadronic final state is required to be well separated in rapidity from the system Y containing the final proton. Furthermore the mass of the system Y, M_Y, is small ($M_Y \leq 1.6$ GeV in the case of H1), and the magnitude of the squared four-momentum transferred at the proton vertex are small ($|t| \leq 1\ GeV^2$ in the case of H1). Cross-sections are presented for the production of two jets, belonging to the system X, each with transverse momentum, $P_t^{jet} \geq 5$ GeV (H1) and $P_t^{jet} \geq 6$ GeV (ZEUS), relative to the photon direction in the rest frame of X . The jet pseudorapidities η^{jet} in the laboratory are restricted to be in the interval $-1.5 \leq \eta^{jet} \leq 1$ (ZEUS) and $-1 \leq \eta^{jet} \leq 2$ (H1). Results are presented for photoproduction, $Q^2 \leq 0.1$ GeV^2 (H1), $Q^2 \leq 4$ GeV^2 (ZEUS) and for electroproduction $7.5 \leq Q^2 \leq 80$ GeV^2 (H1). In the photoproduction case, the cross-section dependence on the fraction of the momentum of the photon participating in the jet production shows evidence for the presence of a resolved as well as a direct-photon component in the hard diffractive scattering. Measurements of the cross-section as a function of the fraction of the momentum of the object participating in the production of the jets are presented and compared to predictions using NLO DGLAP (ZEUS) and LO DGLAP (H1) evolved pomeron parton density parameterisations.

.

I. INTRODUCTION

In diffractive interactions at HERA, high p_T jet production has been observed by the H1 and ZEUS Collaborations in photoproduction ($Q^2 \approx 0$)[1][2] and electroproduction ($Q^2 \geq 10 GeV^2$)[2]. This followed the observation of high p_T jets in diffractive $p\overline{p}$ interactions by the UA8 experiment[3] after the proposal of Ingelman and Schlein [4]. This was the first experimental evidence suggesting a partonic structure for the pomeron. Whereas in UA8 the proton (antiproton) was tagged and its momentum measured online, at HERA the diffractive events are tagged by the absence of activity in the forward detectors. This so called rapidity gap trigger corresponds in nearly 90% of the cases to a single proton going down the beam pipe. The momentum fraction carried by the pomeron, $x_{\mathcal{P}}$, is of the order of $e^{-\eta_{gap}}$, where η_{gap} is the difference between the pseudorapidity of the edge of the gap and the pseudorapidity of the proton[5]. In general, the rapidity gap trigger at HERA permits to study the diffractive scattering both in photoproduction and at large Q^2 using events of the type ep →eXY, where the hadronic systems X and Y are separated by a large region of pseudorapidity devoid of hadronic activity. Both collaborations, H1 and ZEUS, have continued the study of large rapidity gap events. The contribution to the proton structure function of the process ep →eXY, where the mass of the system Y, M_Y, and the magnitude of the squared 4-momentum transfer at the proton vertex, $|t|$, are small has been measured differentially in $x_{\mathcal{P}}$ in terms of a structure function $F_2^{D(3)}(x_{\mathcal{P}}, \beta, Q^2)$ [6][7] where $\beta = x_{Bj}/x_{\mathcal{P}}$. In the following we shall present results obtained by the H1 and the ZEUS collaborations.

.

II. H1 ANALYSIS

A Regge analysis of $F_2^{D(3)}$ [6], extracted from the 1994 H1 data, ($M_Y \leq 1.6 GeV^2$ and $| t | \leq 1 GeV^2$), shows that the pomeron exchange is dominant at small $x_{\mathcal{P}}$, with the exchange of reggeons becoming increasingly important as $x_{\mathcal{P}}$ increases. At the present level of precision, the $x_{\mathcal{P}}$ dependence of the diffractive contribution factorises such that the β and Q^2 dependence of $F_2^{D(3)}$ at a fixed small value of $x_{\mathcal{P}}$ can be considered in terms of the evolution of a structure function for the pomeron. Assuming that the QCD evolution for $\beta \leq 0.65$ is governed by the DGLAP[8] equations, the analysis[6] of $F_2^{D(3)}(x_{\mathcal{P}} = 0.003, \beta, Q^2)$ yields the parton distribution of the pomeron at a scale of 4.5 GeV^2. Under the hypothesis of diffractive factorisation, this parton distribution is expected to universally describe diffractive interactions wherever perturbation theory may be applied. In order to test these ideas, large rapidity gap events that contain a high transverse momentum dijet system in the component X of the hadronic finale state have been investigated in separate analyses of photoproduction and DIS. In effect, the condition $p_T^{jet} > 5$ GeV entails the possibility to make perturbative QCD calculations of the underlying two-body hard interaction processes. Thus, the data could be compared to model based predictions using the pomeron structure function at a scale given by the transverse momentum $\hat{p_T}$ of the outgoing partons. The analyses are performed in the rest frame of the system X, the transverse momenta being defined with respect to the photon direction. The results presented here are based on data obtained in 1994, from the collision of 27.5 GeV positrons with 820 GeV protons, with an integrated luminosity of 2.2 pb^{-1} in photoproduction and $2 pb^{-1}$ in electroproduction. In both cases, the condition $x_{\mathcal{P}} < 0.05$ is imposed, where $x_{\mathcal{P}} = (Q^2 + M_X^2)/(Q^2 + W^2)$. Jets with a transverse momentum cut $p_T \geq 5$ GeV are selected using a cone algorithm with radius R=1 in the $\eta - \varphi$ plane.

A. RESULTS

A total of 400 dijet events are selected in photoproduction, and 55 events in electroproduction. The cuts ($Q^2 \leq 0.01$, $0.25 \leq Y \leq 0.7$, $-1 \leq \eta_{jet} \leq 2$ for photoproduction and $7.5 \leq Q2 \leq 80 GeV^2$, $0.1 \leq Y \leq 0.7$ for electroproduction) ensure a good containment of the system X in the detector. All distributions are corrected for acceptance and smearing effects using Monte Carlo simulations. The Monte Carlo simulations use the programs POMPYT [9] for photoproduction and RAPGAP [10] for electroproduction. Both are based on the factorisation of the jet production cross section into a flux of objects with a partonic structure emitted from the proton, followed by a hard interaction with a photon at a scale chosen in the photoproduction case to be the transverse momentum $\hat{p}_T$ of the partons in the hard process, and in the electroproduction case the photon virtuality. The flux distribution of the exchange is parameterised as a superposition of a pomeron and a meson component, following the analysis of inclusive diffractive data in DIS [6]. The parton content of the pomeron is obtained from a QCD analysis of the same data, and is characterised for $Q^2 \approx 5\ GeV^2$ by a gluon momentum weighted distribution peaking above $x_{g/\mathcal{P}} = 0.9$ ($x_{g/\mathcal{P}}$ is the fraction of the $\mathcal{P}$ momentum carried by the gluon). At the higher scale values of the present analyses radiation tends to flatten this distribution. The meson is modelled following the pion structure function [11], and is thus rapidly decreasing with β (β is the momentum fraction of the exchanged object carried by the struck quark). The POMPYT simulation includes for the photon a resolved and a direct contribution; the latter corresponds to $x_\gamma \simeq 1$, where $x_\gamma = \sum(E - p_z)_{jj} / \sum(E - p_z)^{had}$, the sums extending in the numerator over hadrons forming the jets, and in the denominator over hadrons in the X system. The +z direction is that of the outgoing proton, and that of the pomeron, whereas the photon longitudinal momentum is along the -z direction. The data are compared to the Monte Carlo predictions as a function of p_T^2, x_γ, and $z_{\mathcal{P}}$. The variable $z_{\mathcal{P}}$, defined as $z_{\mathcal{P}} = (Q^2 + M_{jj}^2)/Q^2 + M_X^2)$ where M_{jj} is the invariant mass of the dijet system, is related to the fraction of the pomeron (or meson)momentum carried by the parton participating in the hard interaction. In the case of boson gluon fusion process, it correponds to the momentum fraction carried by the initial gluon. In photoproduction, $z_{\mathcal{P}}$ is reduced to $\sum(E+p_z)_{jj} / \sum(E+p_z)^{had}$. The photoproduction results are displayed in Figs. 1 and 2 where the Monte Carlo predictions for the pomeron and the meson contributions are shown separately. The pomeron contribution dominates over the meson even for $x_{\mathcal{P}} \simeq 0.05$ because of the difference in the parton distributions and the kinematical effects related to the jet requirement. Within the large errors, which do not include the uncertainty on the scale choice, a reasonable agreement is observed with the POMPYT Monte Carlo predictions, both in normalisation and in shape. In contrast, the data are incompatible with a soft parton distribution in the pomeron, parameterised as $\beta \times G(\beta) = 6(1-\beta)^5$ (not shown). The shape of the $z_{\mathcal{P}}$ distribution also disfavours the hypothesis of a “super hard”, non QCD-evolved gluon distribution in the pomeron. As the POMPYT predictions are based on an analysis of inclusive DIS diffractive scattering, the factorisation hypothesis is supported by the present data, within the limits of the measurement precision and the uncertainty inherent in the choice of factorisation scale. The x_γ distribution indicates that both a resolved and a direct photon contribution are required.

The electroproduction results shown in Fig. 3 lead to conclusions similar to photoproduction, both the normalisation and the shape of the data being reasonably described by the RAPGAP Monte Carlo. The $z_{\mathcal{P}}$ distribution is compatible with a dominating photon gluon fusion contribution, with the gluon distribution in the pomeron obtained from inclusive diffractive DIS interactions. Given the large uncertainties, mainly of statistical origin, the data can hardly distinguish between the choice of Q or of $\hat{p_T}$ as the scale for the hard interaction. In conclusion, diffractive dijet production has been studied for $x_{\mathcal{P}} < 0.05$, both in photo- and electroproduction. The data are reasonably well described by Monte Carlo simulations based on the analysis of inclusive diffractive interactions in deep inelastic scattering. This gives support, within the precision of the present measurement, to the hypotheses of a factorisable pomeron flux, accompanied by a meson component, and of a universal pomeron structure function.

III. ZEUS ANALYSIS

Diffractive photoproduction ($Q^2 \approx 0$) of high transverse energy jets, $\gamma p \to$ jet + hadrons + p, provides a process which is sensitive both to the quark (via $\gamma q \to$ qg) and gluon (via $\gamma g \to q\bar{q}$) densities in the pomeron. The measurement of the diffractive sructure function in DIS [7], combined with the measured inclusive jet cross section in diffractive photoproduction gave the first experimental evidence for the gluon content of the pomeron [12]. The measurements of diffractive dijet photoproduction allow the study of the fractional momentum spectrum of the pomeron parton densities and of the underlying two-body hard processes. In leading order two types of processes contribute to jet production : the photon interacts directly with a parton in the pomeron or the photon acts as a source of partons which scatter off those in the pomeron (resolved process). The cross section dependence on the fraction of the photon momentum participating in the production of the two jets, x_γ^{obs} ($\approx x_\gamma$ of H1) is sensitive to the presence of these two components. The measurements of the differential diffractive dijet cross sections have been made as a function of the pseudorapidity (η^{jet}) and the transverse energy of each jet (E_T^{jet}), the γ p centre-of-mass energy (W), x_γ^{obs}, and the fraction of the pomeron momentum (β^{obs}) ($\approx z_{\mathcal{P}}$ of H1) participating in the production of the two jets with highest E_T^{jet}. The data sample used in this analysis was collected with the ZEUS detector at the ep collider during 1994 and corresponds to an integrated luminosity of 2.65 pb^{-1}.

A. DIJET CROSS SECTIONS

Differential dijet cross sections have been measured in the kinematical region defined by $Q^2 \leq 4GeV^2$ and $134 \leq W \leq 277$ GeV with the most-forward going hadron at $\eta_{max} \leq 1.8$. The cross sections refer to jets at the hadron level with cone radius of 1 unit in the $\eta - \varphi$ plane. In all figures the statistical errors are indicated as the inner error bars. The systematic uncertainties not associated with the energy scale of the jets have been added in quadrature to the statistical errors and are shown as the outer error bars. The dominant systematic error, the uncertainty on the energy scale of the jets, is shown as a shaded band in each figure. The contribution from non-diffractive processes to the measured cross sections has been subtracted. Since diffractive hard scattering models account only for processes in which the proton remains intact after the collision, the contribution to the measured cross section from diffractive proton dissotiation has to be taken into account when comparing to model predictions[7]. This contribution also has been removed from the data as an overall subtraction. Diffractive processes were simulated using POMPYT [9]. The parton densities of the pomeron in POMPYT were parameterised according to the form described below. The cross section $d\sigma/dE_T^{jet}$ has been measured in the range of E_T^{jet} between 6 and 14 GeV integrated over $-1.5 \leq \eta^{jet} \leq 1$ and is presented in Fig. 4. The cross section $d\sigma/d\eta^{jet}$, shown in Fig. 5, has been measured in the range $-1.5 \leq \eta^{jet} \leq 1$ integrated over $E_T^{jet} \geq 6$ GeV. The measured cross section $d\sigma/dW$ is shown in Fig. 6. In two-to-two parton scattering, the momenta of the incoming partons can be calculated from the two partons in the final state. Let x_γ and β be the fraction of the photon and pomeron momenta carried by the initial state partons. The variables x_γ and β can be expressed as function of the initial photon momentum, $x_{\mathcal{P}}$, and a sum running over final state parton quantities. Since the partons are not measurable objects, the observable x_γ^{obs} defined in terms of jets was introduced [13]. Its definition is : $x_\gamma^{obs} = \sum_{jets} E_T^{jet} e^{-\eta^{jet}}/(2yE_e)$ where now the sum runs over the two jets of highest E_T^{jet}. Similar considerations lead to the following definition : $\beta^{obs} = \sum_{jets} E_T^{jet} e^{+\eta^{jet}}/(2x_{\mathcal{P}}E_p)$. The variable $x_{\mathcal{P}}$ is calculated using the expression : $x_{\mathcal{P}} = M_X^2/W^2$. The variable β^{obs} represents the fraction of the pomeron's momentum partcipating in the production of the two jets. The cross section $d\sigma/dx_\gamma^{obs}$ has been measured in the x_γ^{obs} range between 0.2 and 1 for dijet production with $E_T^{jet} > 6$ GeV and $-1.5 < \eta^{jet} < 1$. The cross section, shown in Fig. 7, peaks at the high values of x_γ^{obs} with a tail that extends to low x_γ^{obs} values. The comparison of model predictions to the data gives evidence for a resolved and a direct-photon components. The cross section $d\sigma/d\beta^{obs}$ hase been measured in the β^{obs} range between 0.4 and 1 for dijet production with $E_T^{jet} > 6$ GeV and $-1.5 < \eta^{jet} < 1$ and is shown in Fig. 8. The cross section increases as β^{obs} increases and shows that there is a sizeable contribution from those events in which a large fraction of the momentum of the pomeron is invested in the hard scattering.

B. DGLAP ANALYSIS

To improve the precision on the gluonic content of the pomeron stucture function, a combined DGLAP analysis of the ZEUS measurements of the diffractive structure function[7] and of the measured dijet cross sections, presented in the previous subsection, has been performed following the proposal by Collins et al[5]. The diffractive structure function was extracted in the kinematical range of $0.08 \leq y \leq 0.5$, $8 \leq Q^2 \leq 100 GeV^2$, $6.310^{-4} \leq x_{\mathcal{P}} \leq 10^{-2}$ and $0.1 \leq \beta \leq 0.8$ The fits to the DIS data are based on full NLO QCD calculation whereas the fits to the photoproduction data make use of LO QCD calculation (based on POMPYT) and include both direct and resolved processes. The Donnachie and Landshoff [14] pomeron flux factor has been used in both cases. Each of the fits is represented by a parameterisation of the initial distribution at $\mu_0^2 = 4\ GeV^2$ for the $u(\beta,\mu^2)$ $(= \bar{u} = d = \bar{d})$ quark and for the gluon. The c and s quark distributions are assumed to be zero at the initial scale. The parton distributions are evolved in μ^2 according to the DGLAP equations . The scale is set equal to Q for the DIS data and equal to the transverse momentum of the outgoing partons for the photoproduction data. The fits were performed simultaneously to the ZEUS DIS[7] measurements and the dijet cross sections $d\sigma/d\eta^{jet}$, $d\sigma/dE_T^{jet}$, $d\sigma/dW$, and $d\sigma/dx_\gamma^{obs}$. The measured cross section $d\sigma/d\beta^{obs}$ has not been used in the fits. The results of three different fits, using the following parameterisations of the pomeron parton density:

$$\beta \cdot f_{u/\mathcal{P}}(\beta,\mu_0^2) = a_1\beta(1-\beta) + c_1(1-\beta)^2)$$
$$\beta \cdot f_{g/\mathcal{P}}(\beta,\mu_0^2) = 0$$

(labelled as "hard quark + soft quark" in the figures),

$$\beta \cdot f_{u/\mathcal{P}}(\beta,\mu_0^2) = a_2\beta(1-\beta)$$
$$\beta \cdot f_{g/\mathcal{P}}(\beta,\mu_0^2) = b_2\beta(1-\beta)$$

(labelled as "hard quark + hard gluon" in the figures),

$$\beta \cdot f_{u/\mathcal{P}}(\beta,\mu_0^2) = a_3\beta(1-\beta)$$
$$\beta \cdot f_{g/\mathcal{P}}(\beta,\mu_0^2) = b_3\beta^8(1-\beta)^{0.3}$$

(labelled as "hard quark + singular gluon“ in the figures),

where a_i, b_i, c_i are free parameters of the fits, are compared to ZEUS data in Figs 4 to 8. The results of the fit in which the pomeron is assumed to be made exclusively of quarks at the initial scale ($\mu_0^2 = 4\ GeV^2$) is unable to describe simultaneously the measured diffractive structure function and the dijet cross sections in diffractive photoproduction. However, the models 2 and 3 which include a substantial hard momentum component of gluons at the initial scale describe well the shape and normalisation of both sets of measurements. The $d\sigma/d\beta^{obs}$ distribution, which was not included in the fit, shows a preference for the singular gluon distribution. The relative importance of the conributions of resolved and direct processes to $d\sigma/dx_\gamma^{obs}$ has been studied. The contributions from direct (dashed line) and resolved (dot-dashed line) processes, together with their sum (solid line), are shown in Fig. 7. The sum of the contributions from resolved and direct processes gives a good description of the data. The shape of the contribution of either a purely direct-photon or a purely resolved-photon is not able to reproduce the data. A resolved-photon component is needed for values of x_γ^{obs} below 0.8. This represents evidence for the presence of resolved and direc photon components in diffractive dijet photoproduction. In conclusion, the measured cross section $d\sigma/dx_\gamma^{obs}$ as a function of x_γ^{obs}, the fraction of the momentum of the photon participating to the production of the two highest E_T^{jet} jets, peaks at $x_\gamma^{obs} \approx 1$ with a pronounced tail to lower values. The comparison of model predictions to the data provides evidence for resolved and a direct-photon components in diffractive dijet photoproduction. A DGLAP analysis of the measurements of the diffractive structure function in DIS [7] and of the measured cross sections $d\sigma/d\eta^{jet}$, $d\sigma/dE_T^{jet}$, dσ/dW, and $d\sigma/dx_\gamma^{obs}$ presented here has been performed. The pomeron has been assumed to have a hadron-like partonic structure in the form of parton densities which evolve according to DGLAP equations. Fits with different parameterisations of the parton densities at the initial scale $\mu_0^2 = 4\ GeV^2$ to both sets of measurements have been made. The results of a fit in which the pomeron is assumed to be made exclusively of quarks at $\mu_0^2 = 4\ GeV^2$ is do not describe simultaneously the measurements of the diffractive structure function and the dijet cross sections in diffractive photoproduction. However, the models which include a substantial hard momentum component of gluons at $\mu_0^2 = 4\ GeV^2$ describe the shape and normalisation of both sets of measurements well. A measurement of the cross section for dijet diffractive photoproduction as a function of β^{obs} is presented. The measured cross section $d\sigma/d\beta^{obs}$ increases as β^{obs} increases and shows that there is a sizeable contribution to dijet production from those events in which a large fraction of the pomeron's momentum is invested in the hard scattering. The shape of the measured $d\sigma/d\beta^{obs}$ favors a more singular gluon distribution. .

IV. OUTLOOK

New data, with much higher statistics, obtained by both collaborations in 1995, 96, and 97 will permit to put a harder test on the hypothesis of factorisation of the $x_{\mathcal{P}}$ dependence of the diffractive differencial cross section. They will also deepen our insight concerning the the pomeron partonic structure Q^2 dependence. In particular they will help to answer the question whether this dependence is fully described by the parton density DGLAP evolution.

---

[1] T. Ahmed et al.,H1 Coll., Nucl. Phys. B435, 3 (1995);.
M. Derrick et al.,ZEUS Coll. Phys. Lett. B346, 399 (1995);B356, 129 (1995)

[2] M. Derrick et al.,ZEUS Coll. Phys. Lett. B332, 228 (1994)

[3] R. Bonino et al., UA8 Coll., Phys. Lett. B211, 239 (1988);.
A. Brandt et al., UA8 Coll., Phys. Lett. B297, 417 (1992)

[4] G. Ingelman and P. Schlein, Phys. Lett. B152, 256 (1985)

[5] J.C. Collins et al., Phys. Rev. D 51, 3182 (1995)

[6] C.Adloff et al.,H1 Coll.,Z. Phys.C76, 613 (1997)

[7] M.Derrick et al.,ZEUS Coll.,Z. Phys.C68, 569 (1997)

[8] V. N. Gribov,L. N. Lipatov,Sov. J. Nucl. Phys. 15 (1972)438 and 675;.
Yu. Dokshitzer,JETP 46 (1977)641;.
G. Altarelli, G. Parisi,Nucl. Phys. B126, 298 (1977)

[9] P.Bruni and G. Ingelman,Proc. of the Int. Europhys. Conf., Marseille,1993, p. 595

[10] H. Jung, Comp. Phys. Comm. 86,147 (1995)

[11] M. Gluck, E. Reya, A. Vogt,Z. Phys. C53, 651 (1992)

[12] M. Derrick. et al.,ZEUS Coll. Phys. Lett. B356, 129 (1995)

[13] M. Derrick. et al.,ZEUS Coll. Phys. Lett. B322, 287 (1994)

[14] A. Donnachie and P.V. Landshoff,Nucl. Phys. B303 634 (1988);.
A. Donnachie and P.V. Landshoff,Phys. Lett. B285 172 (1992)

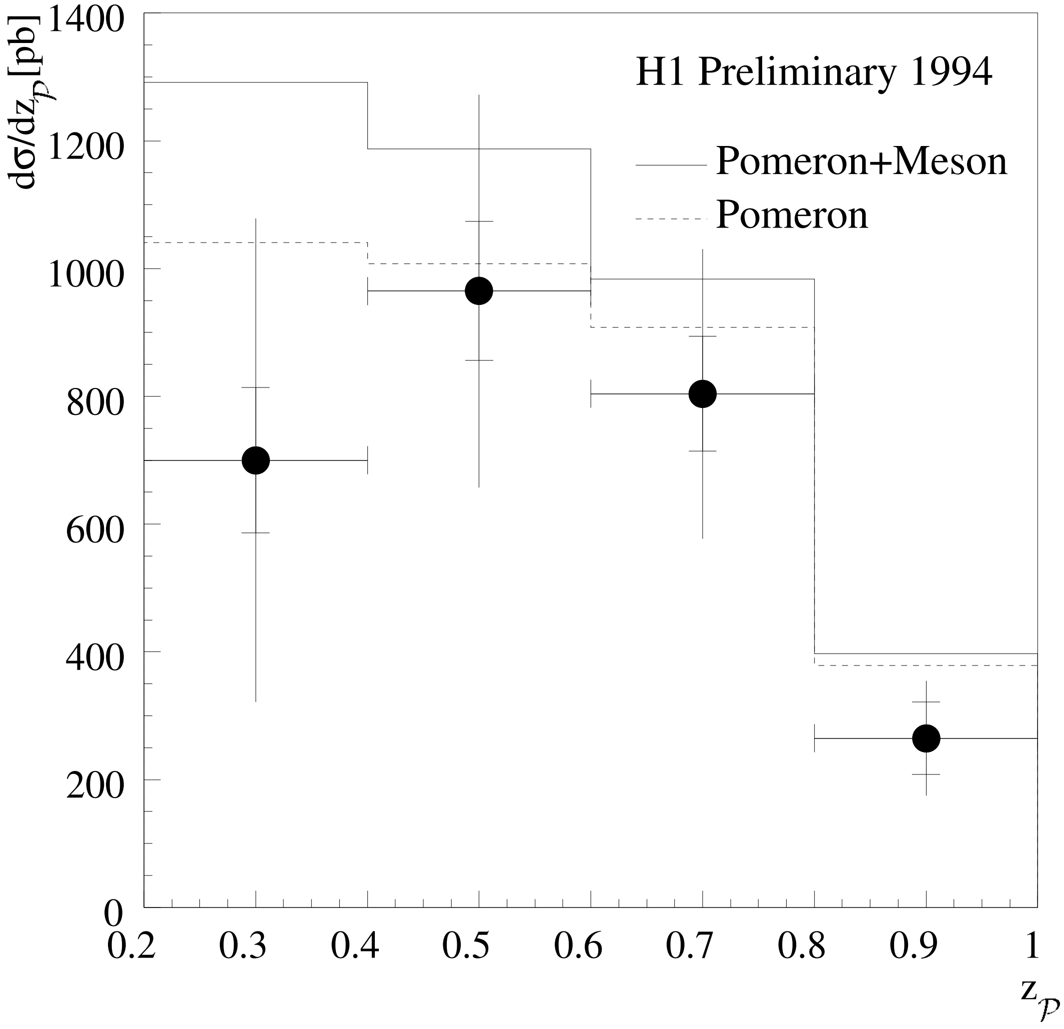

FIG. 1. Di-jet cross section in photoproduction as function of $z_{\mathcal{P}}$.

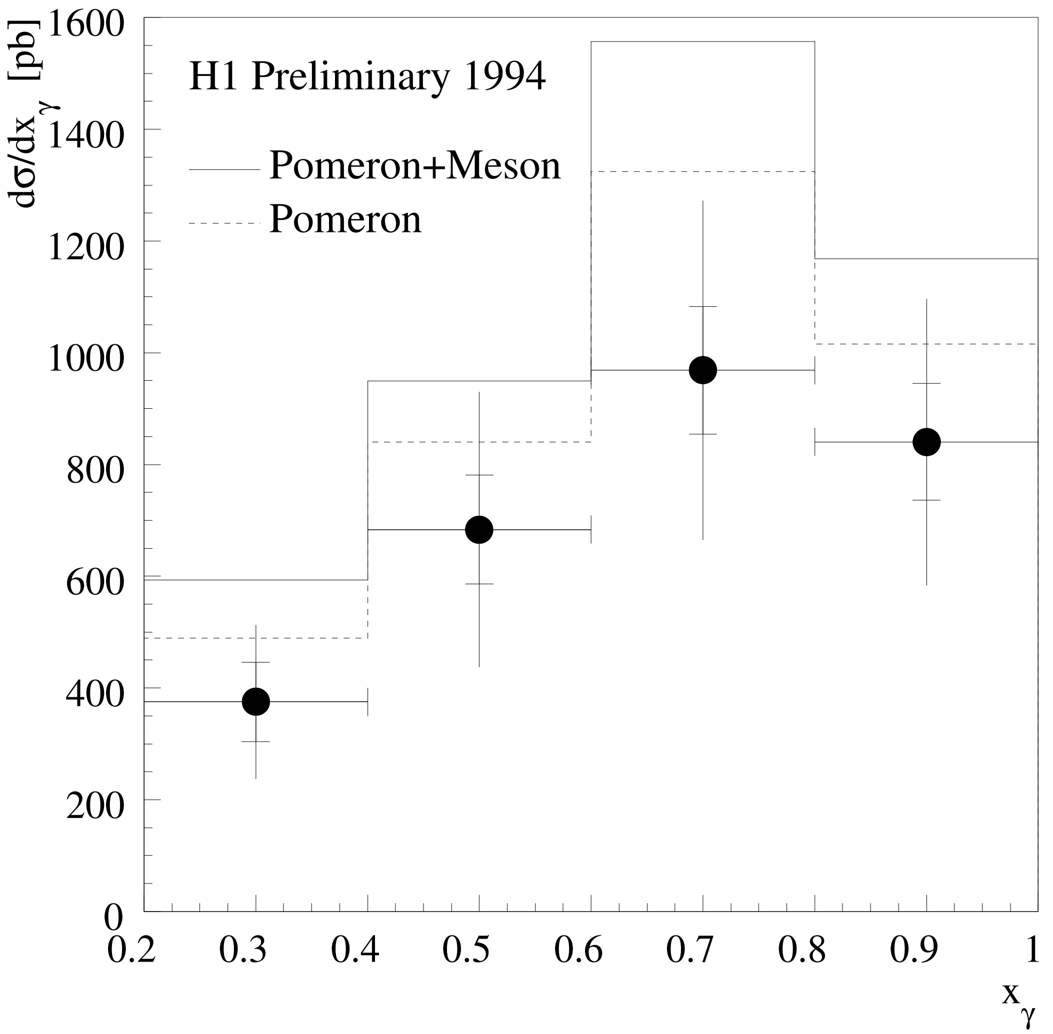

FIG. 2. Di-jet cross section in photoproduction as function of x_γ.

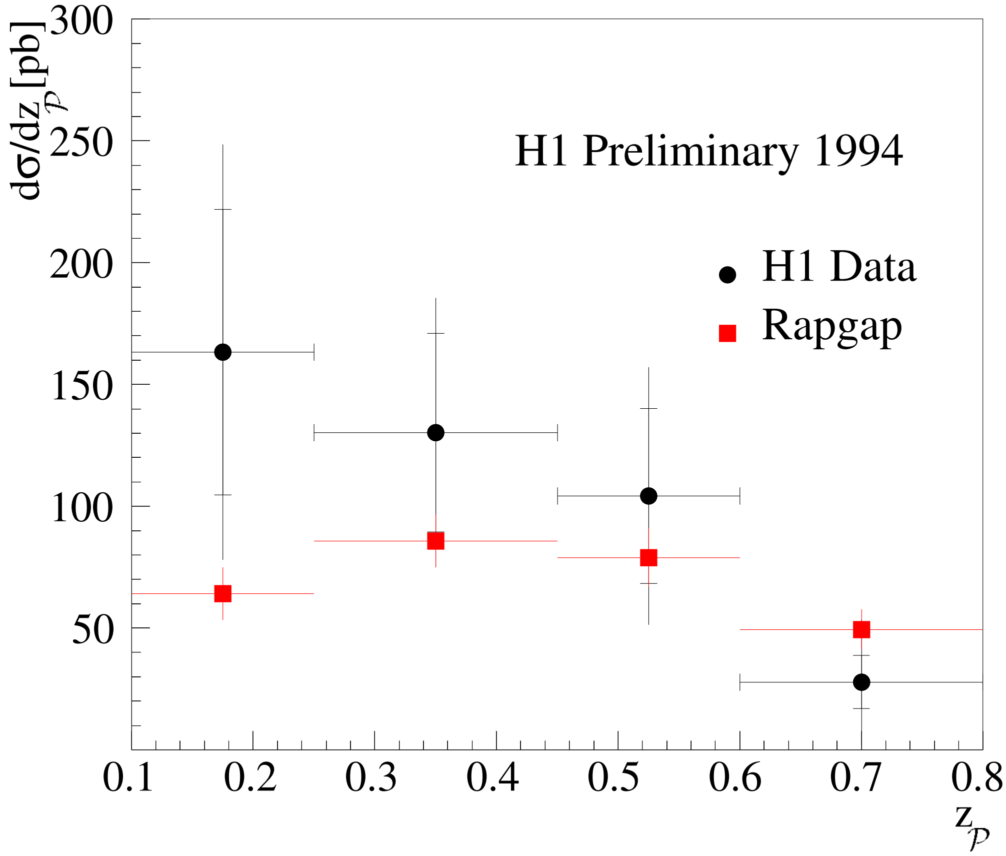

FIG. 3. Di-jet cross section in electroproduction as function of $z_{\mathcal{P}}$.

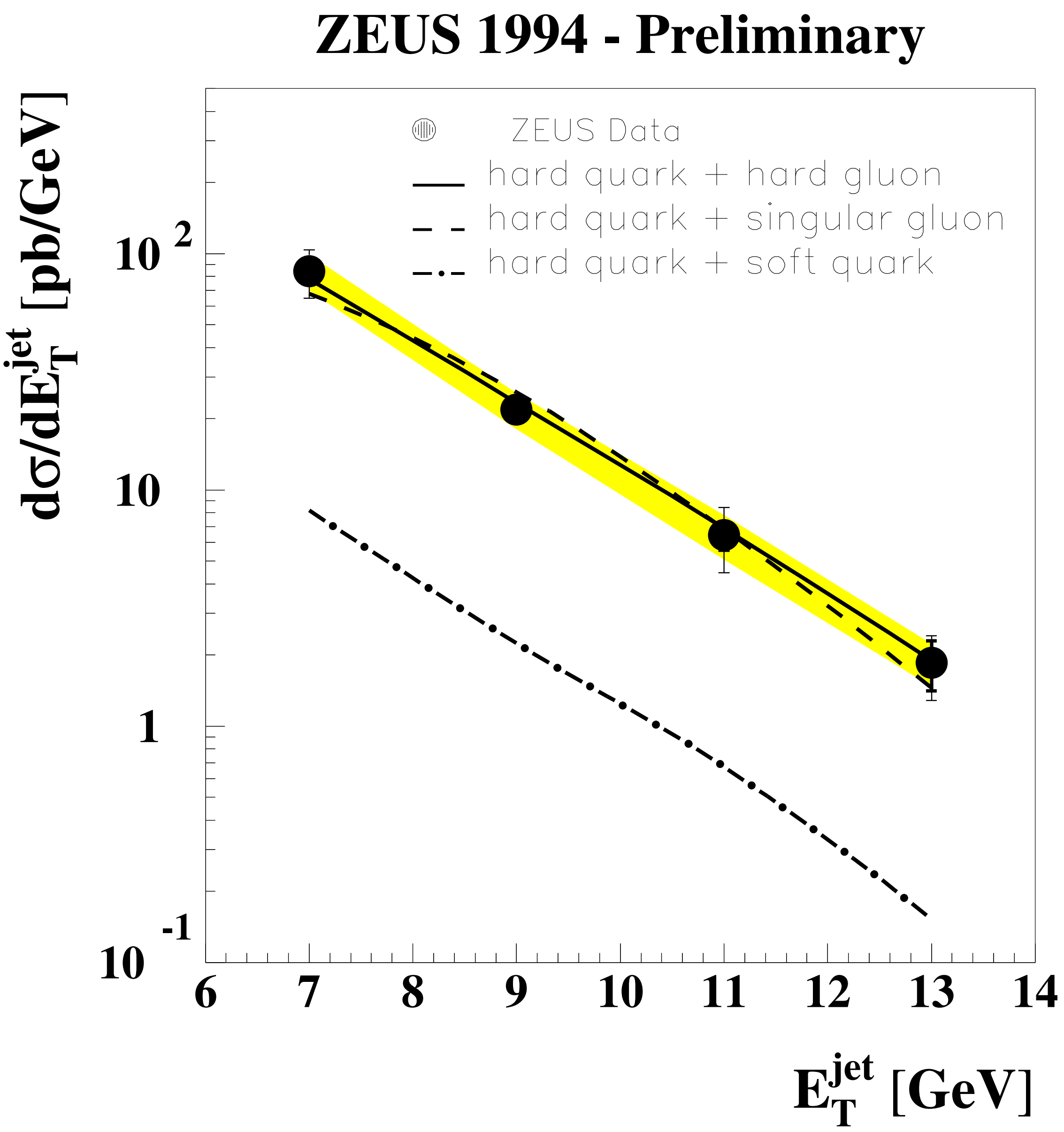

FIG. 4. Measured dijet cross section $d\sigma/dE_T^{jet}$ integrated over -1.5 $\leq \eta^{jet} \leq$ 1 in the kinematic region defined by $Q^2 \leq 4$ GeV^2 and 134 $\leq W \leq$277 GeV with the most-forward going hadron at $\eta_{max} \leq 1.8$(black dots). The inner error bars represent the statistical errors of the data, and the outer error bars show the statistical and systematic uncertaities -not associated with the energy scale of the jets- added in quadrature. The results of the DGLAP fits using different pomeron parton distributions are shown(see text)

.

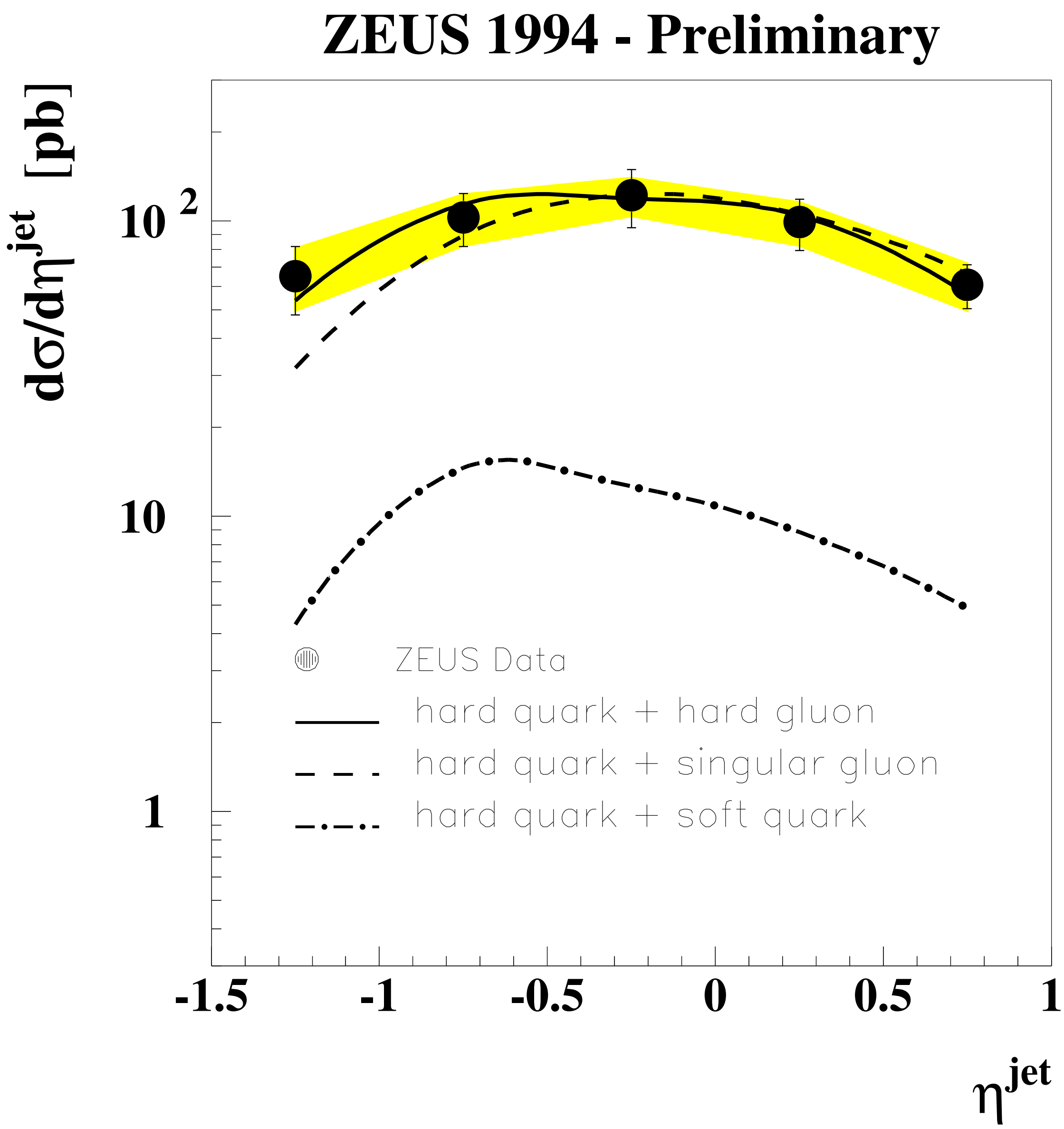

FIG. 5. Measured dijet cross section $d\sigma/d\eta^{jet}$ integrated over $E_T^{jet} \geq 6$ GeV in the kinematic region defined by $Q^2 \leq 4\ GeV^2$ and $134 \leq W \leq 277$ GeV with the most-forward going hadron at $\eta_{max} \leq 1.8$(black dots). The inner error bars represent the statistical errors of the data, and the outer error bars show the statistical and systematic uncertaities -not associated with the energy scale of the jets- added in quadrature. The shaded band displays the uncertainty due to the energy scale of the jets. The results of the DGLAP fits using different pomeron parton distributions are shown(see text)

.

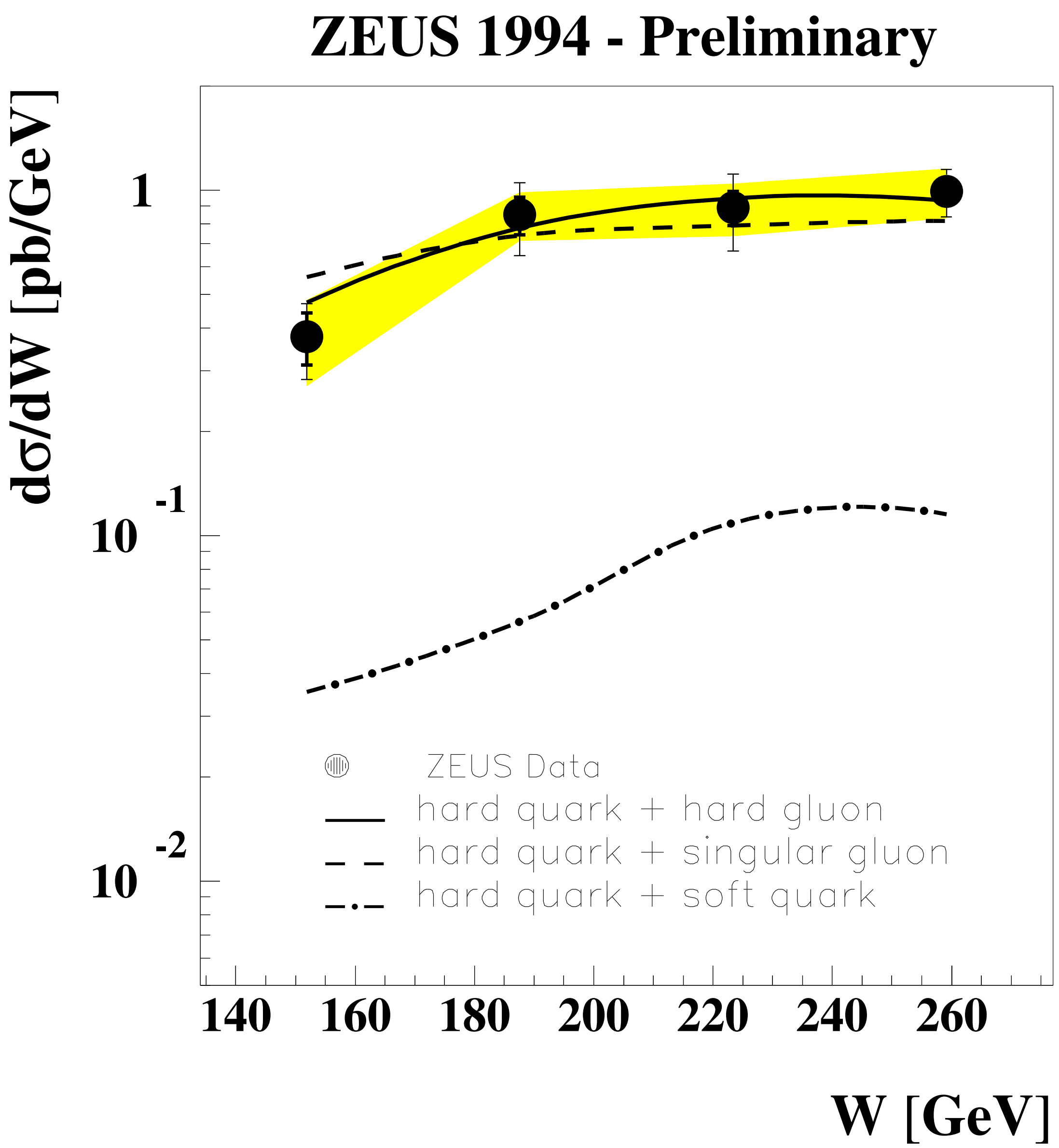

FIG. 6. Measured dijet cross section $d\sigma$/dW integrated over $E_T^{jet} \geq$6 GeV and -1.5 $\leq \eta^{jet} \leq$ 1 in the kinematic region defined by $Q^2 \leq 4\ GeV^2$ and 134 $\leq W \leq$277 GeV with the most-forward going hadron at $\eta_{max} \leq$ 1.8(black dots). The inner error bars represent the statistical errors of the data, and the outer error bars show the statistical and systematic uncertaities -not associated with the energy scale of the jets- added in quadrature. The shaded band displays the uncertainty due to the energy scale of the jets. The results of the DGLAP fits using different pomeron parton distributions are shown(see text)

.

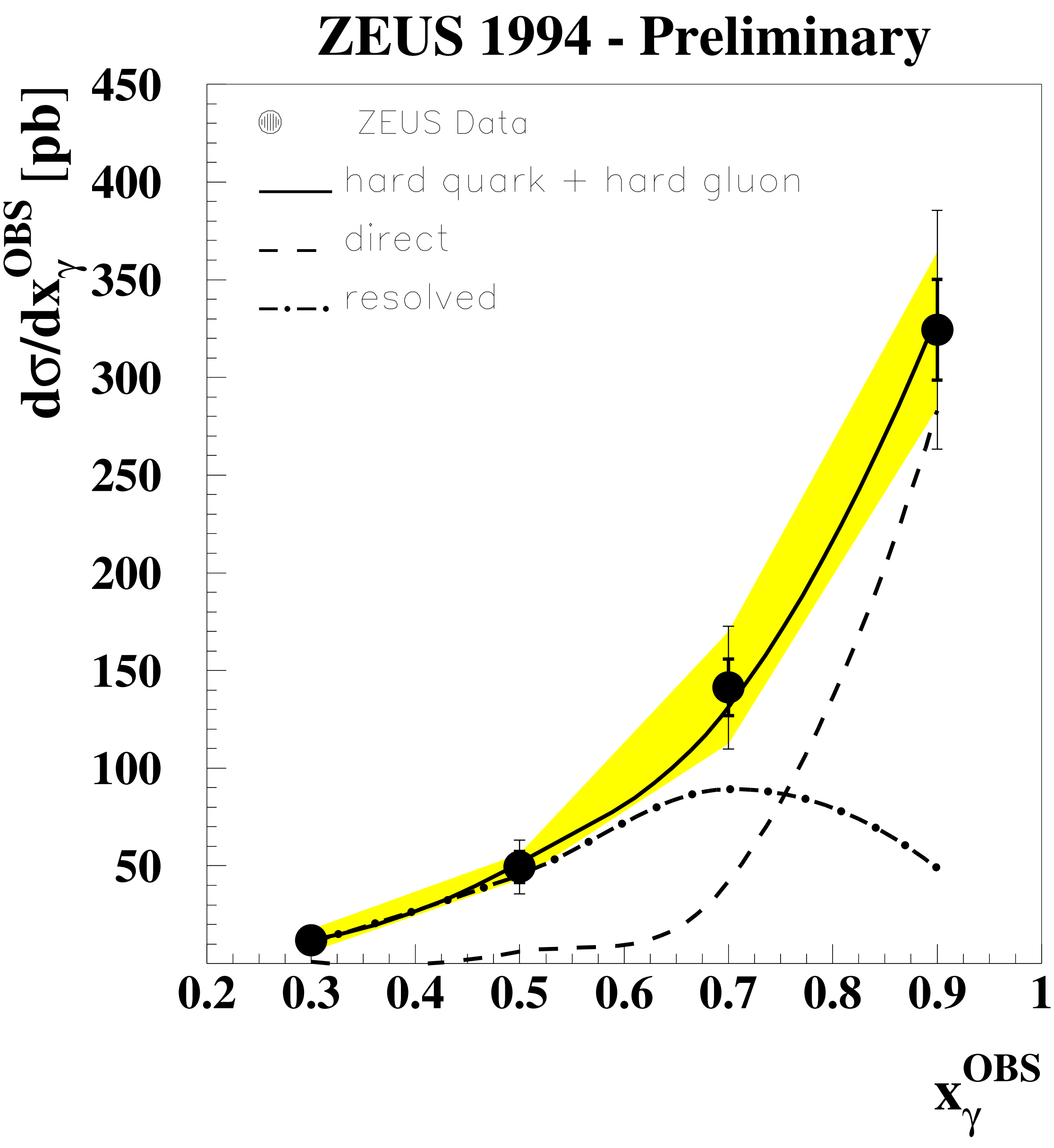

FIG. 7. Measured dijet cross section $d\sigma/dx_\gamma^{obs}$ integrated over E_T^{jet} $\geq$6 GeV and -1.5 $\leq$ η^{jet} $\leq$ 1 in the kinematic region defined by $Q^2 \leq 4$ GeV^2 and 134 $\leq W \leq$277 GeV with the most-forward going hadron at $\eta_{max} \leq 1.8$(black dots). The inner error bars represent the statistical errors of the data, and the outer error bars show the statistical and systematic uncertaities -not associated with the energy scale of the jets- added in quadrature. The shaded band displays the uncertainty due to the energy scale of the jets. The results of the DGLAP fits using different pomeron parton distributions are shown(see text)

.

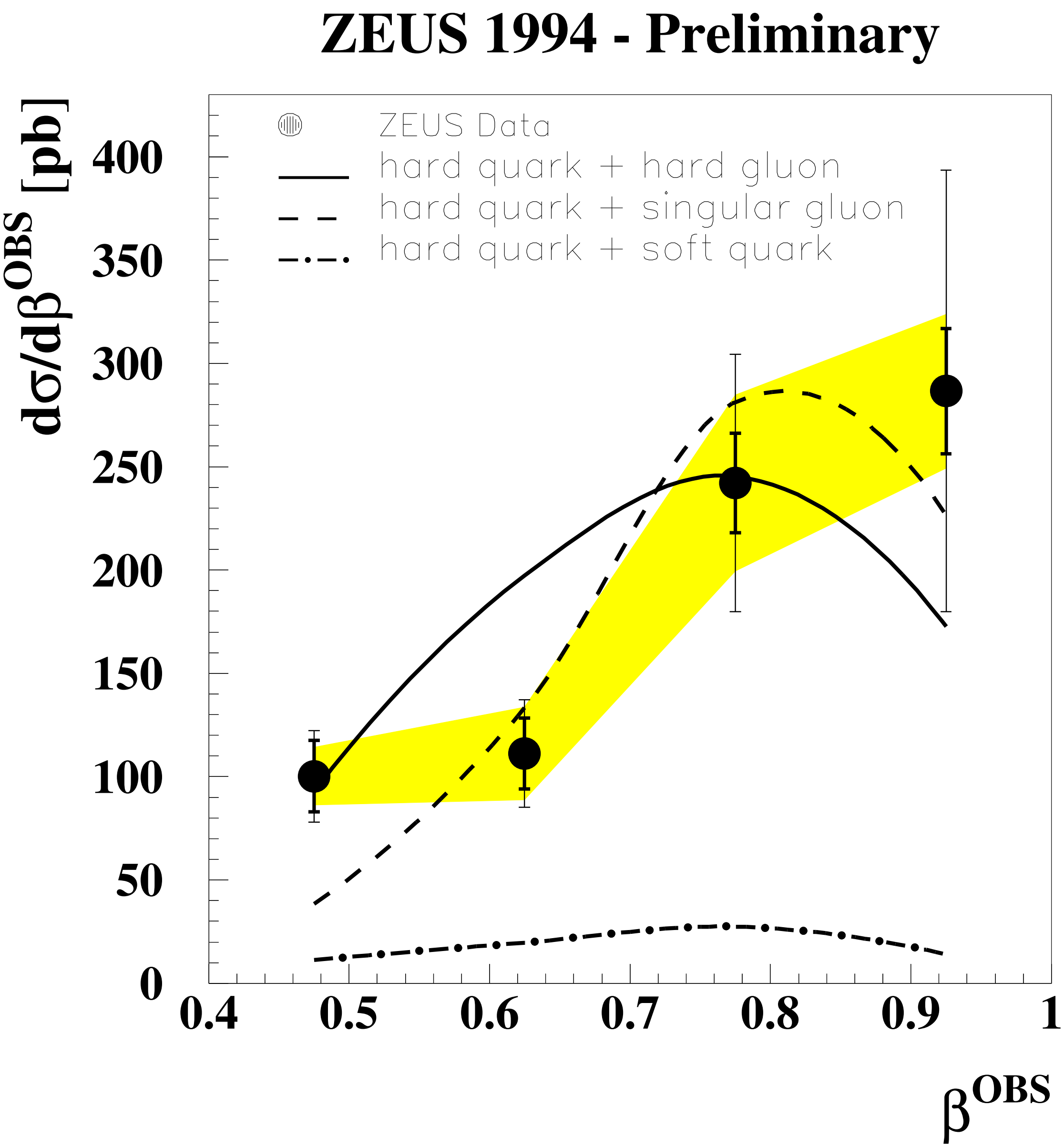

FIG. 8. Measured dijet cross section $d\sigma/d\beta^{obs}$ integrated over E_T^{jet} $\geq$6 GeV and -1.5 $\leq$ η^{jet} $\leq$ 1 in the kinematic region defined by $Q^2 \leq 4\ GeV^2$ and 134 $\leq W \leq$277 GeV with the most-forward going hadron at $\eta_{max} \leq$ 1.8(black dots). The inner error bars represent the statistical errors of the data, and the outer error bars show the statistical and systematic uncertaities -not associated with the energy scale of the jets- added in quadrature. The shaded band displays the uncertainty due to the energy scale of the jets. The results of the DGLAP fits using different pomeron parton distributions are shown(see text)

.